STOCHASTIC CONTINUATION FOR SPACE TRAJECTORY DESIGN

Giacomo Acciarini[(1)], **Nicola Baresi**[(1)], **David Lloyd**[(2)], **Dario Izzo**[(3)]

[(1)]*Surrey Space Center, University of Surrey, GU27XH, Guildford, UK, g.acciarini@surrey.ac.uk, n.baresi@surrey.ac.uk*
[(2)]*Department of Mathematics, University of Surrey, GU27XH, Guildford, UK, d.lloyd@surrey.ac.uk*
[(3)]*Advanced Concepts Team, European Space Agency, Keplerlaan 1, 2201 AZ, Noordwijk, The Netherlands, dario.izzo@esa.int*

ABSTRACT

This paper explores the application of stochastic continuation methods in the context of mission analysis for spacecraft trajectories around libration points in the planar circular restricted three-body problem. Traditional deterministic approaches have limitations in accounting for uncertainties, requiring a two-step process involving Monte Carlo techniques for assessing the robustness of the deterministic design. This might lead to suboptimal solutions and to a long and time-consuming design process. Stochastic continuation methods, which extend numerical continuation techniques to moments of probability density functions, offer a promising alternative. This paper aims to pioneer the application of stochastic continuation procedures in mission analysis, incorporating and acknowledging the stochastic nature of spacecraft missions from the early design phases. By extending existing frameworks to handle fixed points of stroboscopic or Poincaré mappings, the study focuses on robustifying and enhancing trajectory design by considering uncertainties in the determination of periodic orbits. The proposed approach has the potential to discover new solutions that may remain hidden in deterministic analyses, offering improved mission design outcomes. Specifically, this work concentrates on the planar circular restricted three-body problem, assuming uncertainties in both initial conditions and the mass ratio parameter. Stochastic continuation is employed to identify equilibrium points and periodic orbits in this uncertain dynamical system. The generalization of steady states and periodic orbits in uncertain environments is discussed, demonstrating the effectiveness of stochastic continuation in identifying safe operational regions in uncertain astrodynamics problems.

1 INTRODUCTION

Since their discovery, orbits around libration points have been crucial for the design of challenging missions to explore the Sun, the Moon, and other Solar System bodies. While Keplerian dynamics allows us to find a closed-form solution to describe the motion of two bodies due to gravity, it, however, fails to account for the gravitational attraction exerted by other surrounding bodies, and it is therefore not possible to design complex orbits around equilibrium points in this dynamical model. Newton was the first one to discuss the three-body problem, while Lagrange, about 50 years later, found the existence of 5 equilibrium points in a rotating frame describing the circular restricted three-body problem [1]. Other great mathematicians, including Euler and Poincaré, have studied this problem and developed advanced mathematical tools to study interesting phenomena arising in these dynamical systems, including stable and unstable manifolds, periodic orbits, quasi-periodic tori, etc [3]. Nowadays, dynamical systems theory (DST) is the de-facto standard for the qualitative investigation

of these complex solutions and their time evolution. In the last 50 years, periodic orbits have been found and flown in various three-body systems, and natural pathways leading up to those orbits with minimal fuel have been successfully designed using DST techniques [9], [13]–[15], [17], [19], [20]. Numerical continuation techniques have been essential in finding and continuing these periodic and quasi-periodic orbits in three-body environments [16], [24]. However, their application has always been limited to deterministic systems, where it is assumed that the position of the spacecraft and the dynamical model describing its motion are known with infinite accuracy. For this reason, mission analysts typically use Monte Carlo techniques to explore different possible mission scenarios that account for the uncertainties that they face, due to sensor errors, lack of knowledge, etc. This means that the robustness of deterministic trajectories is only assessed a-posteriori and that the whole design process is repeated in case the orbit is not found to be robust enough. While this two-step approach is state-of-the-art, it is a time-consuming process that can potentially lead to sub-optimal trajectories.
Stochastic continuation methods are an emerging class of mathematical techniques that have demonstrated successful results in extending numerical continuation techniques to moments of the probability density function (pdf) of uncertain quantities [26], [29]. This is usually done by calculating fixed points of the corresponding "moment map" of the pdf, which is a low-dimensional map that describes the evolution of the first k moments of the uncertain distribution [22]. Since it is generally not possible to explicitly compute the derivative of fixed points of the moment map, equations-free Newton methods can be used to continue these quantities [21]. This means that the stochastic system does not need to be expressed analytically, but one can simply evolve the system as a computer program, drawing samples from the uncertain distributions and evolving ensembles of trajectories while exploring the uncertainty set. By applying stochastic continuation methods, our aim is to pioneer the application of novel mission analysis methods that include and account for uncertainties since the early mission design phases. Our goal is to apply for the first time stochastic continuation procedures in the context of mission analysis, thereby robustifying, easing, and enhancing the trajectory design process, by incorporating and acknowledging the stochastic nature of spacecraft missions, from the early design phases. In other fields, this has led to the discovery of new interesting solutions that could not be found with the deterministic analysis [22]. While previous work on different fields focused on moment maps of equilibrium points, we plan to extend this to periodic orbits, adapting and improving existing frameworks to handle fixed points of stroboscopic or Poincaré mappings, where the evolution of the satellite is monitored through consecutive surface of section crossings. For this reason, this work is organized as follows: we begin by introducing the relevant literature which covers the dynamical model employed in this study (i.e., the PCR3BP) and the general framework for numerical continuation. Subsequently, in Sec.3, we delve into the stochastic continuation framework, which extends the application of numerical continuation to uncertain dynamical systems. Moving forward, in Sec. 4 and 5, we introduce and discuss the application of stochastic continuation to continue steady states (i.e., equilibrium points) and periodic orbits, in the uncertain PCR3BP scenario. Additionally, we also present test cases to elaborate on the outcomes of employing this technique, which is novel in astrodynamics. Finally, our work concludes in Sec. 6, where we summarize our findings and briefly discuss future prospects.

2 BACKGROUND

2.1 Planar Circular Restricted Three-Body Problem (PCR3BP)

The circular restricted three-body problem (CR3BP) is defined as the problem of three-body when the mass of the third body is negligible (and therefore considered massless) with respect to the two primaries, and when the two primaries move in a circular orbit about the system's barycenter (e.g. the motion of a spacecraft in an orbit in the Earth-Moon system). A particular case of the CR3BP where

the motion of the three bodies happens on a fixed plane is known as the planar circular restricted three-body problem (PCR3BP). We call m_1 and m_2 the masses of the two primaries (i.e., P_1, P_2), while we indicate as P_3 the third massless body, and we normalize the distance by the distance L between P_1 and P_2 (this is also typically referred to as characteristic length), while the time is normalized by the factor: $T = (L^3/G(m_1 + m_2))$ (with G being the gravitational constant). Moreover, the mass ratio parameter is defined as $\mu = m_2/(m_1 + m_2)$, where $m_1 > m_2$ and $\mu \in [0, 1/2]$. We define a rotating frame, $\mathcal{F}_R = (\hat{\mathbf{x}}, \hat{\mathbf{y}})$, which is centered in the barycenter and whose x-axis lies in the P_1-P_2 line, and whose xy-plane represents the same plane where P_2 and P_1 rotate about their barycenter, and where the motion of P_3 takes place. In this reference frame, P_1 is located at $[-\mu, 0]^T$ and P_2 is located at $[(1-\mu), 0]^T$. Indicating with $\mathbf{r} = [x, y]^T$, the position vector of the third body in the rotating frame, and with $\mathbf{r}_{ij}$ the vector that goes from the j^{th} and i^{th} body, we can write:

$$\begin{aligned} \mathbf{r}_{31} &= [x + \mu, y] \\ \mathbf{r}_{32} &= [x - (1-\mu), y] \\ \mathbf{r}_{21} &= [1, 0]. \end{aligned} \tag{1}$$

The motion of the two larger masses is fully determined and assumed to be circular, while the motion of the third particle can be determined via the following set of 2nd-order ordinary differential equations [25]:

$$\begin{aligned} \ddot{x} - 2\dot{y} &= -\frac{\partial \bar{U}}{\partial x} \\ \ddot{y} + 2\dot{x} &= -\frac{\partial \bar{U}}{\partial y}, \end{aligned} \tag{2}$$

where $\bar{U}$ is the augmented (or effective) potential:

$$\bar{U}(x, y, z) = -\frac{1}{2}\big((1-\mu)r_1^2 + \mu r_2^2\big) - \frac{(1-\mu)}{r_1} - \frac{\mu}{r_2}, \tag{3}$$

This set of equations of motion of the CR3BP is Hamiltonian and time-independent. It admits one integral of motion (i.e., a quantity that is conserved through time) [2]. Usually, the celestial mechanics and dynamical astronomy community uses the Jacobi integral, which is defined as:

$$C(x, y, \dot{x}, \dot{y}) = -(\dot{x}^2 + \dot{y}^2) - 2\bar{U}. \tag{4}$$

2.2 Continuation Techniques

Many dynamical systems, including the CR3BP, that depend on one or more parameters can be studied via numerical continuation techniques. These techniques are particularly useful to understand the qualitative changes that occur in the solutions of these systems when parameters are varied. An important application of numerical continuation techniques is the qualitative analysis of non-integrable dynamics systems [3], which involves the study and characterization of equilibrium points (i.e., solutions of the system where the state remains unchanged over time) and/or periodic orbits (i.e., solutions where the system repeats its behavior after a certain period of time) w.r.t. parameters. The implicit function theorem (IFT) is a central pillar behind numerical continuation techniques. It defines the conditions under which families of periodic solutions exist and are unique [10]. This theorem can be paraphrased as follows. Let $\mathbf{G} : \mathbb{R}^n \times \mathbb{R}^m \to \mathbb{R}^n$ satisfy:

1. $\mathbf{G}(\mathbf{x}_0, \mathbf{a}_0) = 0$, with $\mathbf{x}_0 \in \mathbb{R}^n$ and $\mathbf{a}_0 \in \mathbb{R}^m$

2. $DG_x(\mathbf{x}_0, \mathbf{a}_0) \in \mathbb{R}^n \times \mathbb{R}^n$ is nonsingular with bounded inverse (i.e., $||DG_x(\mathbf{x}_0, \mathbf{a}_0)^{-1}|| < M$, for some $M > 0$);

3. $\mathbf{G}$, DG_x are Lipschitz continuous.

Then, there exists a locally unique branch of solutions (i.e., solution family, $\mathbf{x}(\mathbf{a})$) [23].

2.2.1 Numerical Continuation

Having clarified the conditions under which the IFT holds, the numerical continuation framework can be introduced. Assuming a one-dimensional parameter vector (i.e., $\mathbf{a} = a \in \mathbb{R}$), we look for zeros of the vector function: $\mathbf{G}(\mathbf{x}, a) : \mathbb{R}^n \times \mathbb{R} \to \mathbb{R}^n$, and we call a solution to this equation regular if the $n \times (n+1)$ Jacobian matrix of $\mathbf{G}$ w.r.t. $\mathbf{x}$ and a has a maximal rank, n [6]. Then, the IFT ensures that in the neighborhood of this regular solution, a one-dimensional continuum of solutions (where the regular solution belongs), called a solution branch, exists. In this setting, numerical continuation methods refer to a collection of algorithms that utilize strategies to identify these solution curves: a popular continuation algorithm that we also employ in this work is called pseudoarclength continuation.
Keller's pseudoarclength continuation method was introduced to allow the solution branch to be continued past a fold and other degenerate cases [6], [7], [11], [12]. In particular, the idea of this continuation method is to follow a solution branch in a path in the solution space, rather than using a sequence of parameter values. By augmenting the system of equations with an additional equation, the family branch is constrained to lie on a curve in the solution space. This pseudoarclength continuation scheme is displayed in Fig. 1, where its prediction and correction steps are shown.

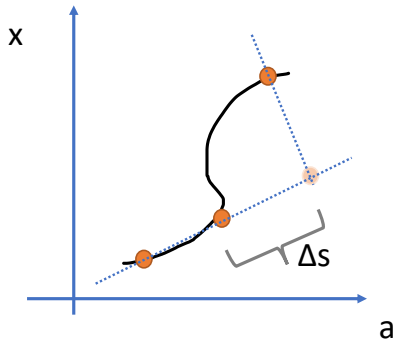

Figure 1: Schematic illustration of pseudoarclength continuation procedure.

Supposing that we have found a regular solution $\mathbf{x}_0, a_0$, and its direction vector $\dot{\mathbf{x}}_0, \dot{a}_0$, pseudoarclength continuation augments the equations to be solved by one:

$$\begin{cases} \mathbf{G}(\mathbf{x}_1, a_1) & = 0 \\ (\mathbf{x}_1 - \mathbf{x}_0)^T \dot{\mathbf{x}}_0 + (a_1 - a_0)\dot{a}_0 - \Delta s & = 0 \end{cases}, \tag{5}$$

where the idea is to parametrize the solution family as a function of the solution curve (i.e., $\mathbf{x}(s), a(s)$), where the family tangent of this solution curve can be written as: $\boldsymbol{\tau} = [d\mathbf{x}/ds, da/ds] = [\dot{\mathbf{x}}, \dot{a}]$. Since we defined the curve as a solution curve, every point on it must satisfy $\mathbf{G} = 0$. Hence, by writing the Taylor expansion of $\mathbf{G}(\mathbf{x}(s + ds), a(s + ds))$, and leveraging the fact that $\mathbf{G}$ is zero on the solution curve (i.e., $G(\mathbf{x}(s), a(s)) = G(\mathbf{x}(s + ds), a(s + ds)) = 0$), we can write:

$$DG_x \frac{d\mathbf{x}}{ds} + DG_a \frac{da}{ds} = (DG_x, DG_a) \cdot \boldsymbol{\tau}^T = 0. \tag{6}$$

Finally, we write the points belonging to a plane perpendicular to the tangent vector at a distance $\Delta s = s - s_0$ from the current solution s_0 as:

$$(\mathbf{x}(s) - \mathbf{x}(s_0), a(s) - a(s_0))^T \boldsymbol{\tau} = \Delta s,$$

which represents the augmented equation in Eq. (5). Moreover, the Jacobian of the augmented equations can be written as:

$$J = \begin{bmatrix} DG_x & DG_a \\ \boldsymbol{\tau} \end{bmatrix}, \tag{7}$$

where from Eq. (6) we know that the tangent vector is orthogonal to the Jacobian of $\mathbf{G}$. Hence, the added equation is linearly independent from the previous set, by definition, therefore not making the Jacobian singular. The tangent vector needs to be updated at each iteration, once convergence is achieved. This can be done using a secant predictor, which consists of the use of the line that intersects the last two found solutions as a family tangent. Then, the new family tangent vector can be used to find the next initial guess for the Newton method, as:

$$\mathbf{x}_1 = \mathbf{x}_0 + \Delta s \, \tilde{\boldsymbol{\tau}}, \tag{8}$$

where $\tilde{\boldsymbol{\tau}}$ is the normalized family tangent vector. Finally, the initial guess can be utilized in a Newton-method scheme to determine the root of $\mathbf{G}$:

$$\mathbf{x}_{k+1,1} = \mathbf{x}_{k,1} - DG_x^{-1}(\mathbf{x}_{k,1})\mathbf{G}(\mathbf{x}_{k,1}). \tag{9}$$

The whole procedure can then be repeated, therefore allowing the exploration of the roots of $\mathbf{G}$ as a function of $\mathbf{x}$ and $\mathbf{a}$.
All these numerical continuation schemes work with the requirements that we can write an explicit equation to find the roots of a function and the Jacobian of such function exists and can be computed or approximated [26]. However, there are cases such as stochastic systems in which these equations are not given explicitly. For continuing these systems, it is necessary to modify the numerical continuation framework. This is done via Jacobian-free Newton-Krylov methods, such as GMRES, which essentially enable the solution of the iterative scheme presented in Eq. 9, without direct access to the Jacobian. In the following section, we introduce stochastic continuation, which is the framework that allows to apply numerical continuation to stochastic systems.

3 STOCHASTIC CONTINUATION

Deterministic systems can be continued using standard numerical continuation techniques (e.g. pseudoarclength continuation), however, when there is the need to deal with uncertain dynamical systems, it is necessary to account for the randomness in the system, due to either uncertainty in the initial conditions, environment parameters, and/or the dynamics. For uncertain initial solutions or parameters, an alternative that is often used is to initially treat the system as a deterministic one and only later investigate deviations from that nominal behavior via Monte Carlo analysis. Whilst this method can lead to acceptable results from an operational standpoint, it can give rise to suboptimal solutions, and can also force one to repeat the deterministic design several times, before converging to a solution that fulfills the constraints, therefore incurring in time losses.
In the last years, the problem of continuing dynamical systems in the presence of uncertainties has been discussed, and a framework for continuing these systems affected by randomness has been developed [29]. This approach has proven effective in various areas, including chemical reaction models and other Hamiltonian systems [22], [29]. Its merit consists in successfully extending the

results of numerical continuation techniques to macroscopic quantities that describe the uncertain distribution. Usually, the operator used to compute these macroscopic quantities is the moment map: this is a deterministic map that describes how the first k moments of the probability density function of the state of a time-varying system evolve through time [22]. Some examples discussed in the literature include the Ising model in two dimensions, a stochastic Swift-Hohenberg model, a one-dimensional stochastic double-well potential, and a two-dimensional heath bath model, among others. These are both partial differential equations and deterministic and stochastic differential equations, with either uncertain or deterministic initial conditions. While these models represent interesting examples of successful applications of stochastic continuation to various dynamical systems, they have only been limited to equilibrium points (i.e., periodic orbits have not been continued) and to low-dimensional systems (i.e., one or two-dimensional dynamical systems).

We assume to have a setup similar to the numerical continuation case, however, in this case, we must distinguish between microscopic and macroscopic quantities. The former, are variables that describe single realizations (i.e., trajectories) of the system, such as the position and velocity vector of a particle, while the latter are those that describe the macroscopic behavior of an ensemble of those particles. Examples of macroscopic quantities are the moments of the distribution of the uncertain quantities, such as the mean, the covariance, and higher-order moments. We assume to have a vector function $\mathbf{G}(\langle\mathbf{x}\rangle, \langle\mathbf{a}\rangle)$, whose zeros are sought, where $\langle\mathbf{x}\rangle$ is the vector of macroscopic quantities (whose corresponding microscopic quantities are referred to as $\mathbf{x}$) and $\langle\mathbf{a}\rangle$ is the vector of macroscopic parameters (whose corresponding microscopic quantities are referred to as $\mathbf{a}$). Furthermore, we use the curly brackets (i.e., $\{\mathbf{x}\}_{i=1}^{n}$, $\{\mathbf{a}\}_{i=1}^{n}$) to indicate an ensemble of microscopic states.

Given a probability density function p of a vector of random variables $\mathbf{x} = [x_1, .., x_n]$, with $\mathbf{x} \in \mathbb{R}^n$, the first k moments of the distribution about the mean can be defined using the expectation operator as:

$$\begin{cases} m_1 & = [\mathbb{E}[x_1], \dots, \mathbb{E}[x_n]] \\ m_{2,ij} & = \mathbb{E}[(x_i - \mathbb{E}[x_i])(x_j - \mathbb{E}[x_j])], \quad \forall i,j = 1, \dots n \\ \dots & \\ m_{k,ij\dots l} & = \mathbb{E}[(x_i - \mathbb{E}[x_i])(x_j - \mathbb{E}[x_j]) \dots (x_l - \mathbb{E}[x_l])], \quad \forall i,j,\dots,l = 1 \dots n \end{cases}, \tag{10}$$

where the expectation operator is given as the n-dimensional integral of the random variable multiplied by the probability density function:

$$\mathbb{E}[x_i] = \int_{\mathbb{R}^n} x_i p(\mathbf{x}) d\mathbf{x}. \tag{11}$$

Thus, the k-th moment of the distribution, m_k, is a tensor of n^k elements.

Our objective is to study the roots of a vector-valued function, $\mathbf{G}$, defined as the difference between the moments after a certain period T, and the moments at the initial time t_0:

$$\mathbf{G} = \begin{bmatrix} m_1(T) - m_1(t_0) \\ m_{2,ij}(T) - m_1(t_0), \ \forall i,j = 1, \dots n \\ \dots \\ m_{k,ij\dots l}(T) - m_{k,ij\dots l}(t_0), \ \forall i,j,\dots l = 1 \dots n \end{bmatrix}, \tag{12}$$

and continue them as a function of the parameters. If we had access to the function $\mathbf{F}$ that regulates the evolution of the macroscopic quantities (e.g. the moments of the distribution), then we could numerically integrate that function and perform numerical continuation on it. However, this is in general not explicitly given, and one relies on the microscopic quantities to probe the behavior of the macroscopic ones [18]. Usually, the relationship between microscopic and macroscopic quantities is of statistical nature (e.g. in the case of the moments of the distribution). Therefore, there needs

to be a procedure from a set of macroscopic quantities that generates the corresponding ensemble of microscopic states, which are evolved at the desired time and then the resulting macroscopic quantities are derived from the propagated ensembles. These three steps are known as lifting, evolving and restricting steps, and are displayed in Fig. 2 [29].

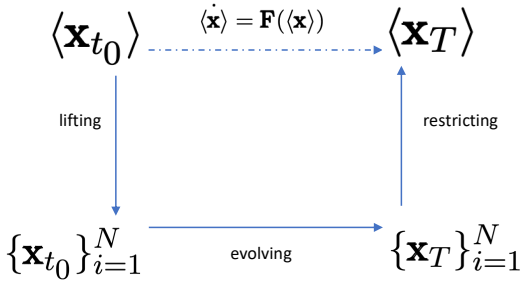

Figure 2: Illustration of lifting, evolving, and restricting operations, which allow computing how macroscopic quantities evolve, without explicit access to the function $\mathbf{F}$.

Once the microscopic quantities are evolved and restricted, one can finally compute the vector-valued function $\mathbf{G}$. In a numerical continuation scheme, Newton's method is then applied to find the next guess, until convergence. However, as already pointed out in Sec. 2.2, for the stochastic case, the function whose zeros are sought is not known explicitly, which also makes the computation of the Jacobian (i.e., DG) not possible analytically, in general. For this reason, to continue stochastic systems, it is helpful to use Jacobian-free Newton-Krylov (JFNK). These are a class of methods that combine Newton's method and Krylov methods [4], to develop a class of algorithms that can apply Newton's algorithm for cases in which the Jacobian matrix of the map cannot be computed analytically [21]. In our case, this is essential because we will be working with moments of a distribution, whose Jacobian is generally not known analytically. In particular, we leverage the generalized minimal residual method (GMRES) to approximate the Jacobian-vector product, without directly having to form the Jacobian [8]. In the following sections, we will discuss the first applications of stochastic continuation in astrodynamics.

4 EQUILIBRIUM POINTS

By reformulating the equations of motion shown in Eq. (2) as a set of four first-order differential equations:

$$\dot{\mathbf{x}} = \mathbf{f}(\mathbf{x}, \mu) = \left[\dot{x}, \dot{y}, -\frac{\partial \bar{U}}{\partial x} + 2\dot{y}, -\frac{\partial \bar{U}}{\partial y} - 2\dot{x}\right]^T, \tag{13}$$

it can be seen that they admit five equilibrium points (i.e., $\mathbf{x}^*$): that is, five points where $\mathbf{f}(\mathbf{x}^*, \mu) = \mathbf{0}$. Moreover, the non-singularity of the Jacobian of $\mathbf{f}$ at those five equilibrium points (i.e., $\nabla \mathbf{f}(\mathbf{x}^*, \mu)$) underscores that a smooth family of solutions $\mathbf{x}^*(\mu)$ exists over the entire domain $\mu \in [0, 0.5]$. While this problem is well understood and thoroughly discussed in the case in which the mass ratio parameter is deterministic, it has not been discussed what happens in an uncertain scenario where μ is described by a probability density function. As a first simple application of stochastic continuation, we formulate the problem for continuing stochastic equilibrium points, which are equilibrium points of the same dynamical system, but assuming that the mass ratio parameter is now uncertain.

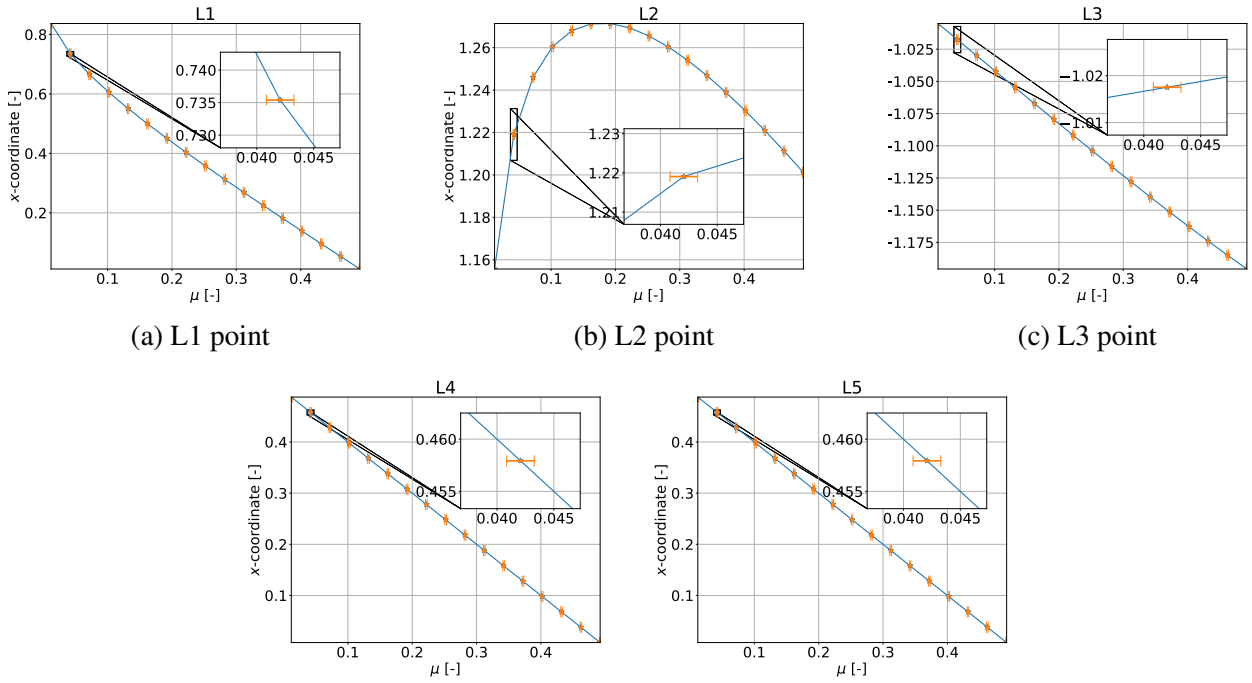

(a) L1 point (b) L2 point (c) L3 point

(d) L4 point (e) L5 point

Figure 3: Stochastic continuation of the five equilibrium points in the PCR3BP.

4.1 First Moment Stochastic Continuation of Equilibrium Points

Following the notation introduced in Sec. 3, the uncertain mass ratio parameter becomes a macroscopic quantity (i.e., $\langle\mu\rangle$), whose microscopic counterparts can be derived by drawing samples from its probability density function: $\mu \sim p(\mu)$. We are interested to find the zeros of the vector-valued function defined as in Eq. (13), however, due to uncertainties in the mass ratio parameter, the vector-valued function belongs to a probability density function, and we reduce the problem to the continuation of its moment. In this case, we only continue the first moment of the distribution. By leveraging the formulation expressed in Eq. (10), this corresponds to:

$$m_1 = \mathbb{E}_\mu[\mathbf{f}(\mathbf{x}, \mu)] \approx \frac{1}{N}\sum_{i=1}^{N}\mathbf{f}(\mathbf{x}, \{\mu\}_i) = 0, \tag{14}$$

Without direct access to the Jacobian of the expected value, which would require the computation of the partial derivatives of the expected value w.r.t. the state and parameter, we draw samples from $p(\mu)$ and we compute the average value of $\mathbf{f}$ using a sample-based approach, then we use a Newton-Krylov GMRES solver to approximate the Jacobian-vector product in order to setup a Newton method that converges towards the stochastic equilibrium.
By using 100,000 samples with a uniform distribution for the mass ratio parameter (with +/-10% as uncertain bounds), and by starting with the Earth-Moon mass ratio parameter, we use the deterministic equilibrium of the Earth-Moon system as initial guess, we use the GMRES method to converge towards the stochastic equilibrium, and then continue the solutions as a function of the mass ratio parameter using pseudoarclength continuation (see Eq. (5)). In Fig. 3, we show the x-coordinate in the rotating system of the equilibrium points in the stochastic (in orange) and deterministic (in blue) case for all five equilibrium points, together with the error bars, which represent the lower and upper bound of the uniform distribution that describes the uncertainty in the mass ratio parameter. As we observe, in this case, the stochastic solution does not lead to the emergence of any particular new dynami-

cal phenomena, but for this mass parameter probability density function, the stochastic equilibrium points seem to closely follow their deterministic counterparts. In particular, we verified that the deterministic and stochastic equilibrium points do not have a significant difference in their position by performing a t-test on the null hypothesis that there is no significant difference between the sample mean and the real mean (where this latter was the equilibrium point of the deterministic system). This was done by computing the mean equilibrium point several different times, with different seeds. The difference in seeds affects the process of drawing samples from the distribution, thereby providing slightly different values for the mean equilibrium points. We can collect these values for different iterations (in our case ten) and compute their mean and standard deviation. Then, by establishing a desired significance level (in our case 0.05) and by applying the t-statistic we could confirm that in our case (for the uniform probability density function we used) we could reject the null hypothesis.

5 PERIODIC ORBITS

While equilibrium points constitute a natural starting point for any differential correction and continuation procedure since they are fundamental concepts in the study of dynamical systems, on the other hand, the mission designer is often interested in the design of periodic orbits. These are solutions that repeat themselves after a certain time period, naturally creating a cyclic behavior, without the need for any extra propellant. The aim of this section is to apply stochastic continuation techniques to the design of periodic orbits. We will first devote Sec. 5.1 and 5.2 to the introduction of Poincaré maps and periodic orbits in the deterministic system, and then, in Sec. 5.3, we will generalize the application of these concepts to uncertain dynamical systems, were we continue the first and second moments of the distribution, demonstrating a new class of solutions that are robust against uncertainties in the environmental parameters and/or initial conditions.

5.1 Surface of Section and Poincaré Maps

A common way to analyze the dynamics of the third body in the circular restricted three-body problem is to discretize the system through the Poincaré map and to use surfaces of section to reduce the dimensionality of the system [25]. A surface of section is a geometric surface in the phase space, that is used to track the motion of the trajectories as they cross it. The simplest example of the surface of section is some coordinate axis (e.g. y=0), but more generically, this is defined as: $S(\mathbf{x}) = 0$.
To be well-defined, it is also required that the trajectory is non-tangent to the surface. Moreover, it is typically required that the flow has some preferred direction of crossing, which can be enforced as: $\frac{\partial S}{\partial \mathbf{x}} \cdot \dot{\mathbf{x}} > 0$.
It is also possible to remove another coordinate (therefore further reducing the dimensionality of the system by one) using the integral of motion. Since we know that the Jacobi constant is conserved during the motion, we can write: $C(\mathbf{x}(t_0)) = C(\mathbf{x}(t)) = \bar{C}$, and remove one of the other coordinates to be integrated. This means that from the original n-dimensional state vector (i.e., $\mathbf{x}$), we are left with $n-2$ reduced state (i.e., $\mathbf{y}$), since two of the coordinates are imposed via $S(\mathbf{x}) = 0$ and $C(\mathbf{x}) = \bar{C}$. This reduced state is mapped (via a nonlinear function of the reduced state: $\mathbf{g}(\mathbf{y}, C)$) to the following surfaces of section with equal Jacobi constant, via a discrete mapping, known as Poincaré map:

$$\mathbf{y}_{i+1} = \mathbf{g}(\mathbf{y}_i; \bar{C}). \tag{15}$$

This map was first introduced by Henri Poincaré [2], and it is extensively used in the computation of periodic orbit, due to its main benefit of reducing the dimensionality of the system.

5.2 Periodic Orbits in the Deterministic System

Defining ϕ as the flow of the dynamical system shown in Eq. (2), then if a periodic orbit exists, with period T, it satisfies $\mathbf{G}(\mathbf{x}_0) = 0$, where:

$$\mathbf{G}(\mathbf{x}_0) = \phi(T, t_0; \mathbf{x}_0) - \mathbf{x}_0 = 0. \tag{16}$$

These equations, together with Eq. (2), define a boundary value problem (BVP), whose solutions can be found via a Newton procedure analogous to the one shown in Eq. (9) [27]. Assuming to start from an initial guess for the vector $\mathbf{x}_0$, which we refer to as $\mathbf{x}_{k,0}$, we can expand via Taylor Eq. (16):

$$\mathbf{G}(\mathbf{x}_{k+1,0}) = \mathbf{G}(\mathbf{x}_{k,0}) + DG(\mathbf{x}_{k,0})(\mathbf{x}_{k+1,0} - \mathbf{x}_{k,0}) + HOT, \tag{17}$$

where DF is the Jacobian of $\mathbf{G}$ w.r.t. the initial conditions and HOT indicate the higher order terms. Ignoring the higher-order terms, rearranging the remaining terms, and inverting the expression in Eq. (17), we can obtain an iterative scheme to find the next iterate, as a function of the previous iterate:

$$\mathbf{x}_{k+1,0} = \mathbf{x}_{k,0} - DG^{-1}(\mathbf{x}_{k,0})\mathbf{G}(\mathbf{x}_{k,0}). \tag{18}$$

This can lead to convergence to a periodic orbit if the Jacobian is invertible and the initial guess is close enough. However, in the CR3BP defined in Eq. (2) all the points along the periodic orbit still satisfy the periodicity condition, and the system is also a Hamiltonian autonomous system, making the periodic orbits organized in one parameter families [28]. These features introduce degeneracies in the BVP, which make the problem ill-posed and not invertible. In order to avoid such degeneracies, periodic orbits can also be found in the reduced system of four-dimensional coordinates, using the Poincaré map defined in Eq. (15). In this setting, periodic orbits are formulated as fixed points of the Poincaré map:

$$\mathbf{G}(\mathbf{y}_0) = \mathbf{g}(\mathbf{y}_0; \bar{C}) - \mathbf{y}_0 = 0, \tag{19}$$

where $\mathbf{y}_0$ is the reduced state of the periodic orbit. In this case, the degeneracies are removed by adding the surface of section and equal Jacobi constant constraints, thereby getting rid of the singularities in the Jacobian computation. Therefore, one can start from an initial guess and setup a Newton procedure to find the roots of Eq. (19) [9]. Finding periodic orbits involves the computation of the Jacobian of the vector-valued function $\mathbf{G}$. However, as already discussed in Sec. 3, this is generally not directly accessible for stochastic systems. For these cases, as already pointed out for the first-moment continuation case, we employ Newton-Krylov methods to approximate the Jacobian-vector product.

5.3 Periodic Orbits in the Stochastic System

Using the same framework of the deterministic case shown in Sec. 5.2, in this case, we assume that both $\mathbf{x}_0$ (i.e., initial conditions) and μ (i.e., the mass ratio parameter) are random variables (due to uncertainties in initial conditions and parameters), which therefore have their associated probability density functions that are defined as $p(\mathbf{x}_0)$ and $p(\mu)$. As explained in Sec. 3, our objective is to continue some macroscopic quantities $\langle \mathbf{x} \rangle$. In particular, we want to find periodic solutions for the macroscopic quantities, which can be defined as zeros of the following vector-valued function:

$$\mathbf{G}(\langle \mathbf{x}_0 \rangle) = \langle \phi_T(\mathbf{x}_0, \mu) \rangle - \langle \mathbf{x}_0 \rangle. \tag{20}$$

Where we use the operator $\langle . \rangle$ to indicate the moment map of the probability density function of the random variables. As we have shown in Eq. (19), the periodic solutions can also be found as fixed points of the Poincaré map. In this case, the system reduces to:

$$\mathbf{G}(\langle \mathbf{y}_0 \rangle) = \langle \mathbf{g}(\mathbf{y}_0, \mu; \bar{C}) \rangle - \langle \mathbf{y}_0 \rangle, \tag{21}$$

where $\bar{C}$ refers to a given fixed value for the Jacobi constant. Due to the extra constraints added by the surface of the section and the equal Jacobi, this latter formulation allows the removal of two equations from the originally four-dimensional system.
Having formulated the vector-valued function whose zeros are sought as in Eq. (21), the stochastic continuation framework in the context of the PCR3BP can be described by the following steps:

1. lifting step: samples are drawn from the probability density functions of both the state and the parameters. We call these ensembles of samples as: $\{\mathbf{y}_0, \mu\}_{i=1}^{N}$, where N is the number of chosen samples;

2. evolving step: for each of the initial states and mass ratio parameter, the final state is computed by integrating the equations of motion of the PCR3BP and using the Poincaré map to reduce the state to two dimensions;

3. restriction step: in a sample-based approach (i.e., where samples are drawn from the probability density function and then propagated individually), it is necessary to compute the macroscopic quantities from the ensemble of propagated trajectories. For instance, the expected value defined in Eq. (11) can be approximated as:

$$\mathbb{E}[y_k(t_f)] \approx \frac{1}{N} \sum_{i=1}^{N} y_k\big(\{\mathbf{y}_0, \mu\}_i\big), \tag{22}$$

where $y_k(t_f)$ is the k-th coordinate of the reduced state after being integrated up to time t_f. This leads to the following approximation for the second moment of the distribution:

$$\begin{aligned}&\mathbb{E}\left[(y_k(t_f) - \mathbb{E}[y_k(t_f)])(y_l(t_f) - \mathbb{E}[y_l(t_f)])\right] \approx \\ &\approx \frac{1}{N} \sum_{i=1}^{N} \left[\left(y_k(\{\mathbf{y}_0, \mu\}_i) - \frac{1}{N} \sum_{i=1}^{N} y_k\big(\{\mathbf{y}_0, \mu\}_i\big) \right) \left(y_l(\{\mathbf{y}_0, \mu\}_i) - \frac{1}{N} \sum_{i=1}^{N} y_l\big(\{\mathbf{y}_0, \mu\}_i\big) \right) \right],\end{aligned} \tag{23}$$

$\forall k, l = 1, \dots n$. As N tends towards infinity, the Central Limit Theorem (CLT) ensures the convergence of the sample mean (i.e., Eq.(22)) towards the analytically computed expected value, provided that the underlying distribution has a bounded variance [5].

Having established the general setup of stochastic continuation for the PCR3BP, we proceeded to perform numerical experiments to verify if such a procedure can work and lead to interesting results. As already mentioned, we limit ourselves to a Poincaré section, which means that we anchor one of the position coordinates to a fixed value, and we find one of the velocity coordinates by imposing a fixed Jacobi constant value. This reduces our state to only one position and one velocity coordinate, thereby leaving us with a two-dimensional reduced state (i.e., $\mathbf{y} = [x, \dot{x}]^T \in \mathbb{R}^2$). We assume that both the initial conditions of the reduced state and the mass ratio parameter are uncertain and can be described by two probability density functions, we assume that the reduced state can be described by a two-dimensional Gaussian distribution (with mean $\bar{\mathbf{y}}_0$ and covariance $\Sigma_{\mathbf{y}_0}$), while the mass ratio parameter is described by a uniform distribution with +/-10% bounds w.r.t. to the mean mass ratio parameter (i.e., $\bar{\mu}$). This can be written as: $\mathbf{y}_0 \sim \mathcal{N}(\bar{\mathbf{y}}_0, \Sigma_{\mathbf{y}_0})$, $\mu \sim \mathcal{U}(\bar{\mu} - \delta\mu, \bar{\mu} + \delta\mu)$.
Our objective is to continue both the first and second moments of the distribution. One possibility would be to directly continue all the independent elements of the covariance matrix terms but this would lead to a formulation that is ill-conditioned (e.g. a zero variance solution would always be a solution of that system). For this reason, we parametrize the covariance matrix using the two axes

of the ellipse (i.e., semi-major and semi-minor axis), which we call a, b, respectively, and the angle between the x-axis and the semi-major axis, which we call θ: note that the area of the ellipse can be found as πab. Then, we express the equations to be continued for the second-moment case as:

$$\mathbf{G}(\bar{\mathbf{y}}_0, \Sigma_{\mathbf{y}_0}) = \mathbf{G}(\bar{\mathbf{y}}_0, a_0, b_0) = \begin{cases} \mathbb{E}_{\mathbf{y}_0,\mu}[\mathbf{y}_f] - \bar{\mathbf{y}}_0 \\ a_f - a_0 \\ \pi a_f b_f - K, \end{cases} \tag{24}$$

where we use the subscripts 0 and f to indicate the initial and final conditions (after a period), respectively, and we use K to refer to the user-defined constant that regulates the area of the final covariance ellipse. By finding the zeros of $\mathbf{G}$, the goal is to find the initial normal distribution of the reduced state that: a) guarantees that the trajectories return, on average, to the same region after one period (i.e., the average of the final distribution has to match the average of the initial distribution, which is a generalization of the periodicity condition for the first moment); b) the variance of these trajectories is bounded and equal to K, and the semi-major axis of the covariance ellipse after one orbit is identical to the initial semi-major axis.

We use the Distant Retrograde Orbit (DRO) family as an initial application of the second moment continuation: our objective is to study what is the stochastic counterpart of this popular family of deterministic periodic orbits in the stochastic case. In particular, within the DRO family, as an initial guess for our stochastic continuation procedure, we choose an orbit that has an initial position vector equal to $\mathbf{r}_{po} = [8.66968844 \times 10^{-2}, 0]^T$, an initial velocity vector equal to $\mathbf{v}_{po} = [1.41842539 \times 10^{-13}, 4.26123697]^T$, and a period of $T_{po} = 6.296488$, all in normalized units. The members of the DRO family have a wide stability region around their periodic orbits, which is a desirable property for many applications since limited perturbations around the initial state stay bounded.

We use 100,000 samples, and we choose as initial covariance an ellipse with the following values: $a = 0.03300155$, $b = 0.0002710345$, $\theta = 1.59089363$ rad. When propagating the set of initial trajectories from these uncertain initial conditions and mass ration parameter, propagating over an orbital period, one would obtain the distributions shown in Fig. 4a, where we show the Poincaré section of the orbits of interest, and we highlight in blue three times the initial covariance ellipse and in orange three times the covariance ellipse after one period.

Instead, the stochastic continuation approach enables us to find solutions that on average return to the same region, and that fulfill the user-defined ellipse area and the same semi-major axis. As an example, we show in Fig. 4c, the Poincaré section of a converged solution with stochastic continuation. There, we display in blue the initial trajectories and three times their covariance, in orange the trajectories after one orbit and three times their covariance, and in black, we also show three times the covariance at each Poincaré section crossing, for a hundred periods. Owing to the DRO stability, we can observe that these solutions preserve bounded covariances centered at the same point for a very long period of time. Once a solution is found, we use the pseudoarclength continuation equation discussed in Eq. (5) to continue the solution at a different period of the orbit. In this way, we are able to extract the family of periodic orbits in the stochastic system. We show a subset of those orbits in Fig. 4b, the ellipse represents the covariance matrix of the converged trajectory, while the center of the ellipse is the converged mean. In the same figure, we also overlap the deterministic solution.

All these solutions have the same property of maintaining the average distribution at the same location after one period, and of fulfilling the abovementioned requirements of the area and the semi-major axis of the ellipse (without the need for any extra propellant). This goes in the direction of locating safe operational regions in chaotic three-body environments with uncertainties. As we observe, these solutions are different than their deterministic counterpart: this highlights that an initial deterministic design with post-processed Monte Carlo analysis might lead to suboptimal solutions w.r.t. a pure stochastic design, with consequent losses of time and costs (e.g. propellant).

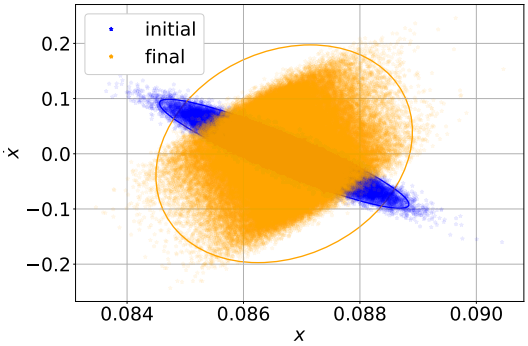

(a) Three times of the initial vs final covariance before stochastic continuation.

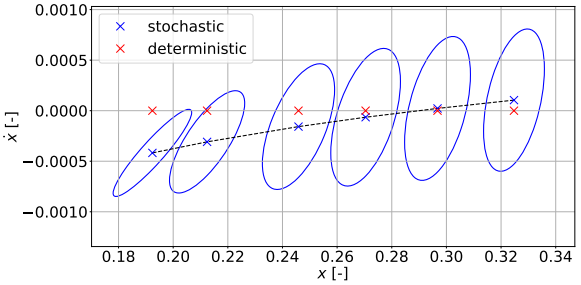

(b) *blue*: solutions found via stochastic continuation (mean and covariance); *red*: deterministic counterparts, for the same Jacobi values.

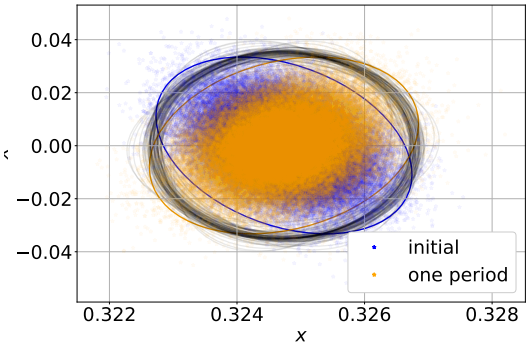

(c) Three times of the initial covariance (in blue), the one after one period (in orange), and Poincaré crossings for 100 periods for a converged solution after stochastic continuation (in black).

Figure 4

6 CONCLUSIONS

Numerical continuation techniques have been essential for the discovery of families of periodic orbits in the CR3BP problem. Their use has allowed us to explore and better understand the chaotic environment of the CR3BP. While very useful for theoretical studies, the reality of spacecraft missions involves many uncertainties in the initial state of the spacecraft.

In our research, we present preliminary results on the utilization of first and second-moment continuation maps. Initially, we employed stochastic continuation to identify and continue equilibrium points within the uncertain PCR3BP. This involved extending the continuation process to encompass the first moments of the probability density function. Subsequently, we extended these techniques to enable the continuation of periodic orbits, incorporating the second moments of the distribution as well. By doing so, we were able to identify regions of safety wherein the spacecraft maintains its operational constraints after one period, while also preserving an average position identical to its initial state. This latter is a generalization of the periodicity condition (on average) for stochastic systems. In these orbits, the spacecraft naturally remains within a bounded region without requiring any additional control. Furthermore, we demonstrated that these orbits deviate from their nominal deterministic counterparts, thus confirming that the current state-of-the-art approach, which involves incorporating uncertainty retrospectively into the design, yields suboptimal solutions.

Although our preliminary findings show promise and indicate the potential for discovering and utiliz-

ing a new class of solutions in practical scenarios that are robust against uncertainties, there are several unresolved inquiries that we intend to address. Specifically, our future investigations will focus on expanding the aforementioned techniques to encompass the CR3BP and extending them to three-dimensional orbits, such as Halo orbits. Subsequently, we aim to apply the developed methodologies to tackle real-world mission challenges.

ACKNOWLEDGMENTS

This work has been funded by the Open Space Innovation Platform (OSIP) of the European Space Agency.

REFERENCES

[1] J.-L. Lagrange, "Essai sur le probleme des trois corps," *Prix de l'académie royale des Sciences de paris*, vol. 9, p. 292, 1772.

[2] H. Poincaré, "Sur le problème des trois corps et les équations de la dynamique," *Acta mathematica*, vol. 13, no. 1, A3–A270, 1890.

[3] H. Poincaré, *Les méthodes nouvelles de la mécanique céleste: Méthodes de MM. Newcomb, Gyldén, Linstadt et Bohlin*. Gauthier-Villars et fils, imprimeurs-libraires, 1893, vol. 2.

[4] M. R. Hestenes, E. Stiefel, *et al.*, "Methods of conjugate gradients for solving linear systems," *Journal of research of the National Bureau of Standards*, vol. 49, no. 6, pp. 409–436, 1952.

[5] B. Gnedenko and A. Kolmogorov, *Limit Distributions for Sums of Independent Random Variables*. Addison-Wesley, 1954.

[6] H. B. Keller, "Numerical solution of bifurcation and nonlinear eigenvalue problem," *Application of bifurcation theory*, 1977.

[7] E. J. Doedel, "Auto: A program for the automatic bifurcation analysis of autonomous systems," *Congr. Numer*, vol. 30, no. 265-284, pp. 25–93, 1981.

[8] Y. Saad and M. H. Schultz, "Gmres: A generalized minimal residual algorithm for solving nonsymmetric linear systems," *SIAM Journal on scientific and statistical computing*, vol. 7, no. 3, pp. 856–869, 1986.

[9] K. C. Howell and H. J. Pernicka, "Numerical determination of lissajous trajectories in the restricted three-body problem," *Celestial mechanics*, vol. 41, no. 1-4, pp. 107–124, 1987.

[10] H. B. Keller, "Lectures on numerical methods in bifurcation problems," *Applied Mathematics*, vol. 217, p. 50, 1987.

[11] E. Doedel, H. B. Keller, and J. P. Kernevez, "Numerical analysis and control of bifurcation problems (i): Bifurcation in finite dimensions," *International journal of bifurcation and chaos*, vol. 1, no. 03, pp. 493–520, 1991.

[12] E. Doedel, H. B. Keller, and J. P. Kernevez, "Numerical analysis and control of bifurcation problems (ii): Bifurcation in infinite dimensions," *International Journal of Bifurcation and Chaos*, vol. 1, no. 04, pp. 745–772, 1991.

[13] K. C. Howell, B. T. Barden, and M. W. Lo, "Application of dynamical systems theory to trajectory design for a libration point mission," *The Journal of the Astronautical Sciences*, vol. 45, pp. 161–178, 1997.

[14] G. Gómez, J. Masdemont, and C. Simó, "Quasihalo orbits associated with libration points," *The Journal of the Astronautical Sciences*, vol. 46, pp. 135–176, 1998.

[15] D. J. Scheeres, "The restricted hill four-body problem with applications to the earth–moon–sun system," *Celestial Mechanics and Dynamical Astronomy*, vol. 70, pp. 75–98, 1998.

[16] W. S. Koon, M. W. Lo, J. E. Marsden, and S. D. Ross, "Dynamical systems, the three-body problem and space mission design," in *Equadiff 99: (In 2 Volumes)*, World Scientific, 2000, pp. 1167–1181.

[17] W. S. Koon, M. W. Lo, J. E. Marsden, and S. D. Ross, "Heteroclinic connections between periodic orbits and resonance transitions in celestial mechanics," *Chaos: An Interdisciplinary Journal of Nonlinear Science*, vol. 10, no. 2, pp. 427–469, 2000.

[18] C. Theodoropoulos, Y.-H. Qian, and I. G. Kevrekidis, ""coarse" stability and bifurcation analysis using time-steppers: A reaction-diffusion example," *Proceedings of the National Academy of Sciences*, vol. 97, no. 18, pp. 9840–9843, 2000.

[19] G. Gómez, W. S. Koon, M. W. Lo, J. E. Marsden, J. Masdemont, and S. D. Ross, *Invariant manifolds, the spatial three-body problem and space mission design*. American Astronautical Society, 2001.

[20] W. S. Koon, J. E. Marsden, and S. D. Ross, "Constructing a low energy transfer," in *Celestial Mechanics: Dedicated to Donald Saari for His 60th Birthday: Proceedings of an International Conference on Celestial Mechanics, December 15-19, 1999, Northwestern University, Evanston, Illinois*, American Mathematical Soc., vol. 292, 2002, p. 129.

[21] D. A. Knoll and D. E. Keyes, "Jacobian-free newton–krylov methods: A survey of approaches and applications," *Journal of Computational Physics*, vol. 193, no. 2, pp. 357–397, 2004.

[22] D. Barkley, I. G. Kevrekidis, and A. M. Stuart, "The moment map: Nonlinear dynamics of density evolution via a few moments," *SIAM Journal on Applied Dynamical Systems*, vol. 5, no. 3, pp. 403–434, 2006.

[23] B. Krauskopf, H. M. Osinga, and J. Galán-Vioque, *Numerical continuation methods for dynamical systems*. Springer, 2007, vol. 2.

[24] R. Seydel, *Practical bifurcation and stability analysis*. Springer Science & Business Media, 2009, vol. 5.

[25] D. J. Scheeres, *Orbital motion in strongly perturbed environments: applications to asteroid, comet and planetary satellite orbiters*. Springer, 2016.

[26] S. A. Thomas, D. J. Lloyd, and A. C. Skeldon, "Equation-free analysis of agent-based models and systematic parameter determination," *Physica A: Statistical Mechanics and its Applications*, vol. 464, pp. 27–53, 2016.

[27] N. Baresi, "Spacecraft formation flight on quasi-periodic invariant tori," Ph.D. dissertation, Department of Aerospace Engineering Sciences, University of Colorado Boulder, Boulder, CO, 2017.

[28] K. R. Meyer and D. C. Offin, "Hamiltonian systems," in *Introduction to Hamiltonian Dynamical Systems and the N-Body Problem*. Cham: Springer International Publishing, 2017, pp. 29–60.

[29] C. Willers, U. Thiele, A. J. Archer, D. J. Lloyd, and O. Kamps, "Adaptive stochastic continuation with a modified lifting procedure applied to complex systems," *Physical Review E*, vol. 102, no. 3, p. 032 210, 2020.